Journal of Science and Transport Technology
Journal homepage: https://jstt.vn/index.php/en

Nonlinear buckling responses of radially pressured FG-GPLRC toroidal shell segments

Luu Ngoc Quang[1], Nguyen Thi Phuong[2,3*]
[1]Faculty of Civil Engineering, University of Transport Technology, Hanoi 10000, Vietnam
[2]Computational Laboratory for Advanced Materials and Structures, Advanced Institute of Materials Science, Ton Duc Thang University, Ho Chi Minh City 70000, Vietnam
[3]Faculty of Civil Engineering, Ton Duc Thang University, Ho Chi Minh City 70000, Vietnam

Article info
Type of article:
Original research paper

DOI:
https://doi.org/10.58845/jstt.utt.2023.en.3.2.19-25

***Corresponding author:**
E-mail address:
nguyenthiphuong@tdtu.edu.vn

Received: 08/05/2023
Revised: 26/06/2023
Accepted: 28/06/2023

Abstract: An analytical approach for nonlinear buckling of functionally graded graphene platelet reinforced composite toroidal shell segments is presented in this paper. The Ritz energy procedure is executed, and radial pressure–deflection expression is constituted to obtain the postbuckling strength and critical buckling pressure of the shells. Significant influences on the buckling responses of shells with three different material distribution rules and mass fractions of graphene platelet, and geometrical dimensions are exemplified and in numerical examples.

Keywords: Nonlinear buckling, Toroidal shell segment, FG-GPLRC, Radially pressured shell, Ritz energy method.

1. Introduction

Functionally graded materials (FGMs) are new kinds of composites with outstanding thermo-mechanic parameters which change continuously and smoothly through the thickness of the structures. In the last decade, studies on the mechanical responses of FGM cylindrical shells have been a common subject. A lot of reports focus on the investigations of the mechanical responses of cylindrical shells made by FGM. Shen and Noda [1] and Shen et al. [2] investigated the postbuckling behavior of FGM hybrid [1] and FGM [2] higher-order shear deformable cylindrical shells under radially external [1] and internal pressures [2] using the perturbation method. The linear buckling responses of FGM cylindrical shells subjected to axially and radially combined compression were also investigated [3]. By using the shear deformation theories, Sofiyev and Hui [4] presented the investigations of the vibration and buckling of FGM cylindrical shells under radial pressure with mixed boundary conditions. Phuong et al. [5] and Nam et al. [6] developed an improved Lekhnitskii's technique for spiral FGM stiffeners and investigated the nonlinear buckling responses of spirally stiffened cylindrical shells under torsional loads and radial pressure, respectively.

With their transcendent material parameters, nanocomposites have attracted significant attention from a number of authors in the world. Two typical nanocomposites are functionally graded carbon nanotube-reinforced composites (FG-CNTRCs), and functionally graded graphene platelet reinforced composites (FG-GPLRCs).

Based on the FGM idea, these new materials are respectively formed by reinforcing the carbon nanotube (CNT), and graphene platelet (GPL) in the isotropic matrix. Shen [7] and Kiani et al. [8] studied the postbuckling and free vibration of FG-CNTRC cylindrical shells and skew cylindrical shells using the perturbation method and Chebyshev-Ritz formulations, respectively. The linear buckling and vibration of shear deformable FG-GPLRC cylindrical shells with eccentric rotating were also investigated [9]. For toroidal shell segments, the nonlinear thermomechanical and mechanical buckling problems of FG-CNTRC shells and FG-CNTRC shells with auxetic core were mentioned using the Donnell shell theory and Galerkin method [10,11].

Clearly that there are no works on nonlinear buckling responses of radially pressured FG-GPLRC toroidal shell segments applying the Ritz energy method from the above references. By using an analytical approach, the nonlinear buckling responses of FG-GPLRC toroidal shell segments are mentioned in this paper. The thin shell theory and large deflection nonlinearities are used and the Ritz energy procedure is executed, the expressions of radial pressure-nonlinear deflection amplitude and maximum deflection-nonlinear deflection amplitude are obtained to determine the postbuckling curve and critical buckling pressure of the shells. Numerical examples validate the significant effects on the nonlinear buckling behavior of shells with UD, FG-X, and FG-O distribution laws, different mass fractions of GPL, and geometrical dimensions.

2. Radially pressured FG-GPLRC toroidal shell segments and stability equations

An FG-GPLRC longitudinally shallow curvature toroidal shell segment is considered. The shell is under the uniformly distributed radial pressure load q (in Pa). R, a, L and h are respectively the circumferential radius, longitudinal radius, shell length and shell thickness. The coordinate system of the shell is chosen as in Figure 1, where the Stein and McEmain approximation is applied to simplify the complex system to a quasi-Cartesian system.

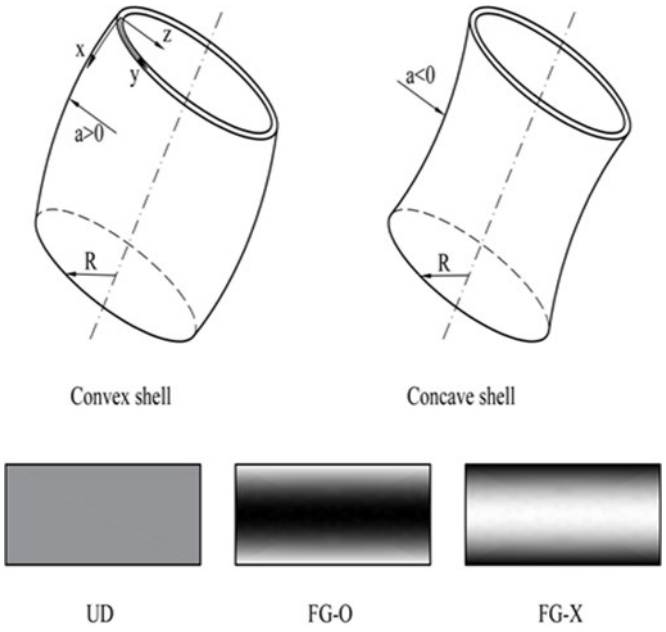

Fig 1. Configuration of radially pressured FG-GPLRC toroidal shell segments

The Young modulus of GPLRC shells can be calculated using the modified Halpin-Tsai technique, presented by [12].

$$E=\left(\frac{3}{8}\frac{1+V_{GPL}\xi_1\lambda_1}{1-V_{GPL}\lambda_1}+\frac{5}{8}\frac{1+V_{GPL}\xi_2\lambda_2}{1-V_{GPL}\lambda_2}\right)E_m, \tag{1}$$

where

$$\lambda_1=\frac{(E_{GPL}/E_m)-1}{\xi_1+(E_{GPL}/E_m)},\ \xi_1=2\left(\frac{a_{GPL}}{t_{GPL}}\right),$$
$$\lambda_2=\frac{(E_{GPL}/E_m)-1}{\xi_2+(E_{GPL}/E_m)},\ \xi_2=2\left(\frac{b_{GPL}}{t_{GPL}}\right), \tag{2}$$

with a_{GPL} is GPL length, b_{GPL} is GPL width, t_{GPL} is GPL thickness. E_m is elastic modulus of matrix, E_{GPL} is elastic modulus of GPL.

The GPL volume fraction V_{GPL} $(V_m+V_{GPL}=1)$, defined as [12]

$$V_{GPL}(z)=\frac{W_{GPL}}{(1-W_{GPL})(\rho_{GPL}/\rho_m)+W_{GPL}}, \tag{3}$$

where ρ_m is density of matrix, ρ_{GPL} is density of GPL.

The mass fraction of GPL W_{GPL} which depends on three popular distribution laws of GPL of shells (see Figure 2) with the following functions [12]

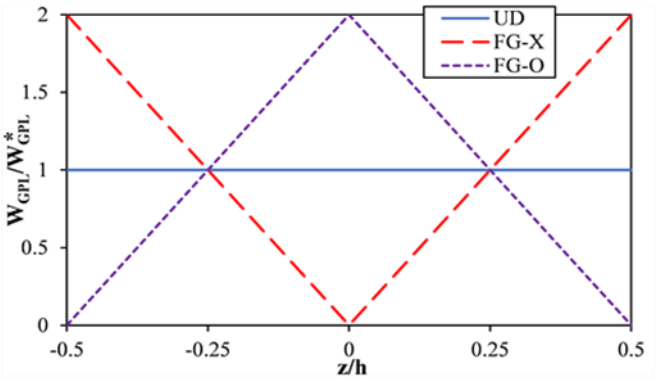

Fig 2. The GPL mass fraction in the directional thickness of shells

$$W_{GPL}(z)=\begin{cases} W^*_{GPL} \text{ for UD-GPLRC,} \\ 4W^*_{GPL}\dfrac{|z|}{h} \text{ for FG-X-GPLRC,} \\ 2W^*_{GPL}\left(1-2\dfrac{|z|}{h}\right) \text{for FG-O-GPLRC,} \end{cases} \quad (4)$$

where the total mass fraction of GPL is denoted by W^*_{GPL}, and $(-h/2 \le z \le h/2)$.

The Poisson's ratio is determined using the classical mixture rule as [12]

$$\nu(z)=(1-V_{GPL})\nu_m+V_{GPL}\nu_{GPL}, \quad (5)$$

The forces and moments can be presented according to the forms

$$\begin{aligned} N_x &= A_{11}\varepsilon_x^0+A_{12}\varepsilon_y^0, \\ N_y &= A_{21}\varepsilon_x^0+A_{22}\varepsilon_y^0, N_{xy}=A_{66}\gamma_{xy}^0, \\ M_x &= -D_{11}w_{,xx}-D_{12}w_{,xx}, \\ M_y &= -D_{21}w_{,xx}-D_{22}w_{,yy}, \\ M_{xy} &= -2D_{66}w_{,xy}, \end{aligned} \quad (6)$$

The stress function φ can be used as the conditions

$$N_y=\varphi_{,xx}, \quad N_{xy}=-\varphi_{,xy}, \quad N_x=\varphi_{,yy}. \quad (7)$$

The deformation compatibility equation of FG-GPLRC shells is presented by [10,11]

$$\begin{aligned} &A^*_{21}\varphi_{,xxxx}+\left(A^*_{11}+A^*_{22}+A^*_{66}\right)\varphi_{,xxyy}+\frac{1}{R}w_{,xx} \\ &+A^*_{12}\varphi_{,yyyy}+\frac{1}{a}w_{,yy}-w^2_{,xy}+w_{,xx}w_{,yy}=0, \end{aligned} \quad (8)$$

Circumferential closed condition for closed shells is expressed by [5,6]

$$\begin{aligned} &\int_0^{2\pi R}\int_0^{L} v_{,y}dxdy \\ &=\int_0^{2\pi R}\int_0^{L}\left(\frac{1}{2}w^2_{,y}+\frac{w}{R}+\varepsilon_y^0\right)dxdy=0. \end{aligned} \quad (9)$$

The total potential energy of the shells is determined as

$$\begin{aligned} \Theta=\frac{1}{2}\int_0^{2\pi R}\int_0^{L}\Big[&\left(\varepsilon_x^0N_x+\gamma_{xy}^0N_{xy}+\varepsilon_y^0N_y\right. \\ &-M_xw_{,xx}-2M_{xy}w_{,xy} \\ &\left.-M_yw_{,yy}\right)-2qw\Big]dxdy. \end{aligned} \quad (10)$$

3. Explicit solutions

Consider a toroidal shell segments under uniformly distributed radial pressure with two simply-supported ends. The deflection form satisfying the simply-supported boundary condition is modeled in the average form, as [5,6]

$$\begin{aligned} w(x,y)=f_0+f_1\sin\left(\frac{m\pi}{L}x\right)\sin\left(\frac{n}{R}y\right) \\ +f_2\sin^2\left(\frac{m\pi}{L}x\right), \end{aligned} \quad (11)$$

where m and n are the positive integer numbers that present the buckling modes of the shells.

The stress function can be calculated by combining Equation (11) and Equation (8). Equation (10) is rewritten by three deflection amplitude, then, the Ritz energy method is applied, i.e.

$$\frac{\partial\Theta}{\partial f_0}=\frac{\partial\Theta}{\partial f_1}=\frac{\partial\Theta}{\partial f_2}=0. \quad (12)$$

Taking into account Equation (9), Equation (12) leads to

$$\zeta_{11}f_0 + \zeta_{12}f_1^2 + \zeta_{13}f_2 - 2q = 0, \quad (13)$$

$$\zeta_{21}f_0 + \zeta_{22}f_1^2 + \zeta_{23}f_2^2 + \zeta_{24}f_2 + \zeta_{25} = 0, \quad (14)$$

$$\zeta_{31}f_0 + \zeta_{32}f_1^2 + \zeta_{33}f_2f_1^2 + \zeta_{34}f_2 - q = 0. \quad (15)$$

The relation between f_0 with f_2 and f_1 with f_2 can be determined from (13-14), as

$$f_1^2 = \left[\zeta_{23}\zeta_{11}f_2^2 + (\zeta_{11}\zeta_{24} - \zeta_{13}\zeta_{21})f_2 + 2\zeta_{21}q + \zeta_{11}\zeta_{25}\right]U, \quad (16)$$

$$f_0 = -\left[\zeta_{12}\zeta_{23}f_2^2 + (\zeta_{12}\zeta_{24} - \zeta_{13}\zeta_{22})f_2 + \zeta_{12}\zeta_{25} + \zeta_{22}q\right]U, \quad (17)$$

$$U = \zeta_{12}\zeta_{21} - \zeta_{11}\zeta_{22}.$$

From Equation (11), by totaling three amplitudes, the maximal deflection of shells is presented, as

$$W_{\max} = f_0 + f_1 + f_2 = -\left[\zeta_{12}\zeta_{23}f_2^2 + (\zeta_{12}\zeta_{24} - \zeta_{13}\zeta_{22})f_2 + \zeta_{12}\zeta_{25} + \zeta_{22}q\right]U + \left[\zeta_{23}\zeta_{11}f_2^2 + (\zeta_{11}\zeta_{24} - \zeta_{13}\zeta_{21})f_2 + 2\zeta_{21}q + \zeta_{11}\zeta_{25}\right]U + f_2, \quad (18)$$

The relation between q with f_2 is obtained from the Equations (13) and (14), presented in the form

$$q = -\frac{\kappa_{11}f_2^3 + \kappa_{12}f_2^2 + \kappa_{13}f_2 + \kappa_{16}}{\kappa_{14}f_2 + \kappa_{15}}. \quad (19)$$

The $q - W_{\max}/h$ postbuckling curves can be obtained by combining Equations (18) and (19) with different f_2.

The upper critical buckling for the shells can be obtained by applying $f_2 \to 0$ in Equations (19), expressed by

$$q^{upper} = -\kappa_{16}/\kappa_{15}. \quad (20)$$

4. Numerical examples

The critical buckling pressures of sandwich FGM cylindrical shells are confronted with those of Nam et al. [6] to verify the accuracy of the present work in Table 1. The work of Nam et al. [6] used the Galerkin method and the nonlinear classical shell theory. The comparison shows that the exact agreements can be observed.

The material parameters of FG-GPLRC are chosen according to the work of Wang et al. [12] in this paper.

The critical buckling pressures of the FG-GPLRC toroidal shell segments and cylindrical shells with various GPL distribution rules and different mass fractions of GPL are presented in Table 2. The significant distinctions in the critical buckling pressures can be indicated with the various distribution rules. Convex, cylindrical, and concave shells are considered and their critical pressures also decrease in this corresponding order. The GPL mass fraction strongly influences the critical load of all three types of shells and three types of distribution laws. With only 1% of the GPL mass fraction also gives an outstanding advantage in terms of the critical pressure of shell segments

The observed investigations show that, for both concave, convex, and cylindrical shells, the critical pressure of buckling phenomenon of FG-X shell is greater than that of UD shell. It can be explained that although with the same volume of GPL for both three distribution laws, GPL is more distributed in the two shell surfaces for FG-X shells, this distribution increases the stiffnesses of the shells, thereby increasing the critical load of buckling phenomenon.

Effects of the mass fraction of GPL on the nonlinear postbuckling bearing capacity of shell segments can be observed in Fig. 3a. Clearly, the postbuckling strength of toroidal shell segments increases largely when the mass fraction of GPL increases, and it seems that the insignificant change in snap-through intensity toroidal shell segments is received.

Postbuckling bearing capacity of toroidal shell segments with convex and concave cases and with different GPL distribution laws are presented in Fig. 3b. The investigations show that the snap-through buckling can be distinctly

observed in the cases of convex shells, oppositely, the slight snap-through intensity can be observed in the cases of concave shell segments.

Influences of a/R ratio on the postbuckling bearing capacities of shells are presented in Figs. 3c,d. For convex toroidal shell segments, the postbuckling bearing capacities of shells increase if the a/R ratio decreases, oppositely, for concave toroidal shell segments, the postbuckling bearing capacities of shell segments increase if the a/R ratio increases. Figures 3e,f present the influences of R/h ratio on the postbuckling bearing capacities of FG-X-GPLRC and FG-O-GPLRC toroidal shell segments, respectively. The investigations present that the postbuckling bearing capacities clearly increase if the R/h ratio increases.

Table 1. Comparisons of critical pressure of buckling phenomenon for sandwich FGM cylindrical shells with the reported work ($h = 0.005$ m, $L/R = 2$, $R/h = 100$)

	Volume fraction index of FGM			
	$k = 0.2$	$k = 1$	$k = 2$	$k = 10$
Nam et al. [6]	1.1474(1,6)*	1.3672(1,6)	1.4519(1,6)	1.5334(1,6)
Present	1.1474(1,6)	1.3672(1,6)	1.4519(1,6)	1.5334(1,6)

*The modes of buckling are in the parentheses (m,n).

Table 2. Critical buckling pressures (MPa) of FG-GPLRC toroidal shell segments and cylindrical shells ($L = 0.75$m, $h = 0.01$m, $R = 0.5$m)

a (m)	GPL distribution	W^*_{GPL}				
		0.002	0.004	0.006	0.008	0.01
5 (Convex shell)	FG-X	8.32(1,6)	9.34(1,6)	10.32(1,6)	11.27(2,6)	12.19(1,6)
	UD	8.08(1,6)	8.86(1,6)	9.62(1,6)	10.35(1,6)	11.06(1,6)
	FG-O	7.81(1,7)	8.28(1,7)	8.75(1,7)	9.20(1,7)	9.64(1,6)
∞ (Cylindrical shell)	FG-X	6.12(1,6)	6.92(1,6)	7.70(1,6)	8.45(1,6)	9.17(1,6)
	UD	5.88(1,6)	6.45(1,6)	6.99(1,6)	7.53(1,6)	8.04(1,6)
	FG-O	5.64(1,6)	5.97(1,6)	6.29(1,6)	6.60(1,6)	6.90(1,6)
-5 (Concave shell)	FG-X	4.42(1,5)	5.01(1,5)	5.57(1,5)	6.12(1,5)	6.65(1,5)
	UD	4.24(1,5)	4.64(1,5)	5.04(1,5)	5.42(1,5)	5.79(1,5)
	FG-O	4.05(1,5)	4.28(1,5)	4.50(1,5)	4.71(1,5)	4.92(1,5)

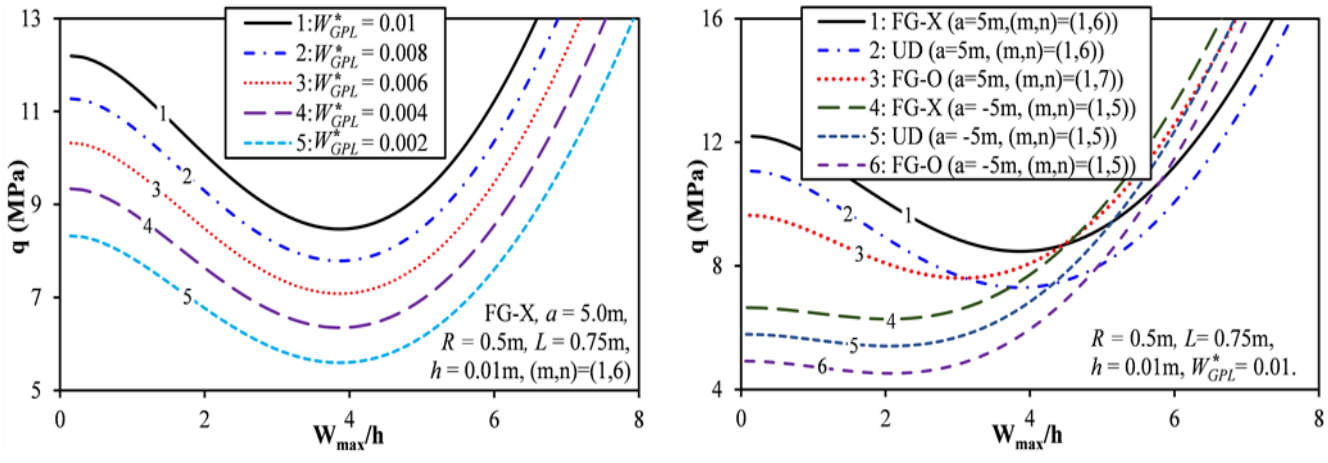

(a) (b)

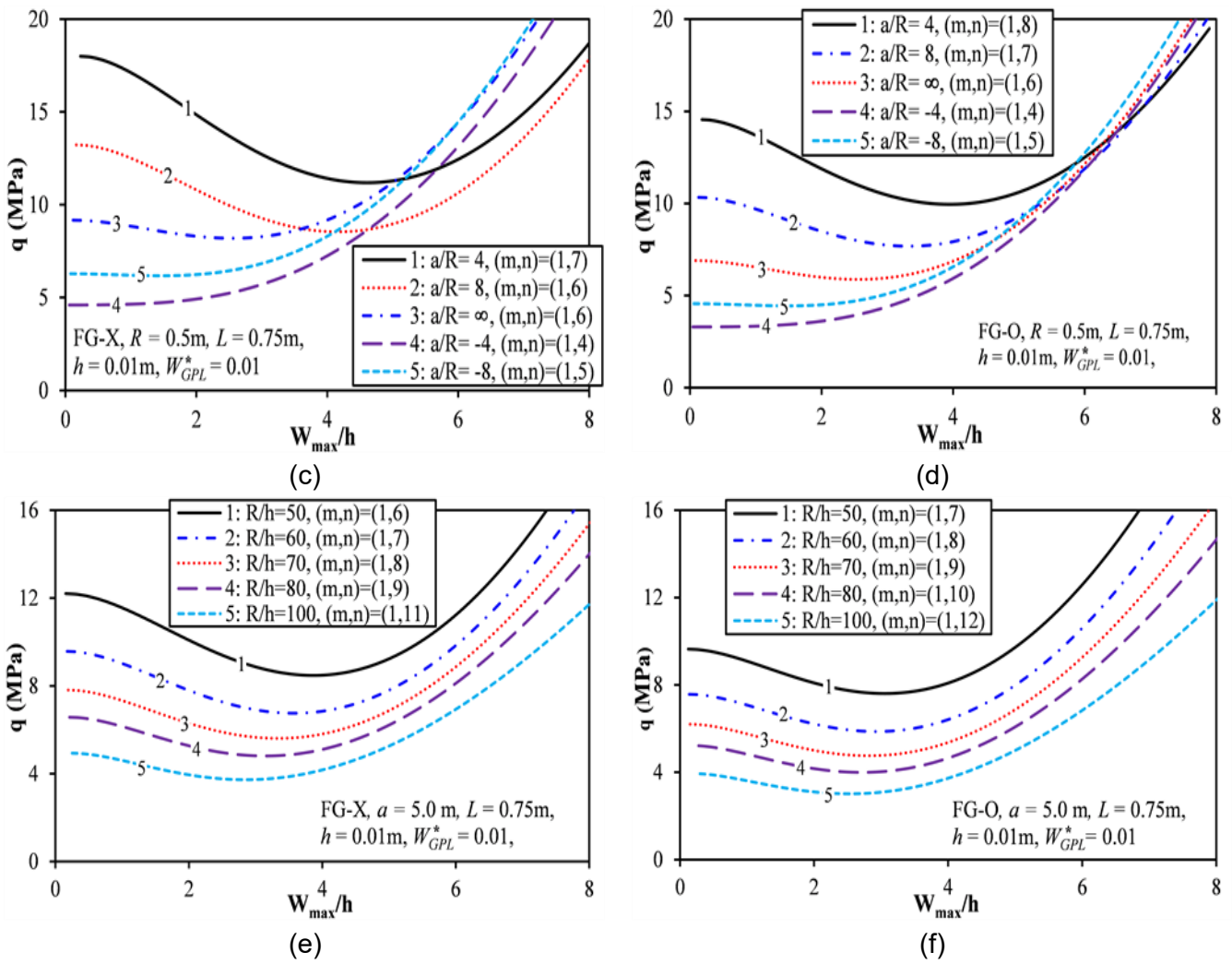

Fig 3. Effects of mass fractions, distribution laws of GPL, and geometric parameters on the postbuckling strength of shells

5. Conclusion

The present work reports an analytical method of the buckling problem of radially pressured FG-GPLRC toroidal shell segments. Ritz energy procedure and Donnell shell theory are applied and the explicit results of postbuckling and critical buckling behavior are obtained. Numerically investigated examples presents the increase of the GPL mass fraction causes the postbuckling strength and critical buckling pressure to increase for both three distribution laws of FG-O, FG-X, and UD. The large influences of geometrical parameters on the buckling responses of shell segments can be also showed from the numerical examples.

References

[1] H.S. Shen, N. Noda. (2007). Postbuckling of pressure-loaded FGM hybrid cylindrical shells in thermal environments. *Composite Structures*, 77(4) 546-560.

[2] H.S. Shen, J. Yang, S. Kitipornchai. (2010). Postbuckling of internal pressure loaded FGM cylindrical shells surrounded by an elastic medium. *European Journal of Mechanics – A/ Solids*, 29(3), 448-460.

[3] E. Bagherizadeh, Y. Kiani, M.R. Eslami. (2011). Mechanical buckling of functionally graded material cylindrical shells surrounded by Pasternak elastic foundation. *Composite Structures*, 93(11), 3063-3071.

[4] A.H. Sofiyev, D. Hui. (2019). On the vibration and stability of FGM cylindrical shells under external pressures with mixed boundary

conditions by using FOSDT. *Thin-Walled Structures*, 134, 419-427.

[5] N.T. Phuong, D.T. Luan, V.H. Nam, P.T. Hieu. (2019). Nonlinear approach on torsional buckling and postbuckling of functionally graded cylindrical shells reinforced by orthogonal and spiral stiffeners in thermal environment. *Proceedings of the Institution of Mechanical Engineers, Part C: Journal of Mechanical Engineering Science*, 233(6), 2091-2106.

[6] V.H. Nam, N.T. Phuong, C.V. Doan, N.T. Trung. (2019). Nonlinear Thermo-Mechanical Stability Analysis of Eccentrically Spiral Stiffened Sandwich Functionally Graded Cylindrical Shells Subjected to External Pressure. *International Journal of Applied Mechanics*, 11(05), 1950045.

[7] H.S. Shen. (2011). Postbuckling of nanotube-reinforced composite cylindrical shells in thermal environments, Part II: pressure-loaded shells. *Composite Structures*, 93(10), 2496-2503.

[8] Y. Kiani, R. Dimitri, F. Tornabene. (2018). Free vibration of FG-CNT reinforced composite skew cylindrical shells using the Chebyshev-Ritz formulation. *Composites Part B: Engineering*, 147, 169-177.

[9] S.W. Yang, Y.X. Hao, W. Zhang, L. Yang, L.T. Liu. (2021). Free vibration and buckling of eccentric rotating FG-GPLRC cylindrical shell using first-order shear deformation theory. *Composite Structures*, 263, 113728.

[10] P.T. Hieu, H.V. Tung. (2019). Thermomechanical nonlinear buckling of pressure-loaded carbon nanotube reinforced composite toroidal shell segment surrounded by an elastic medium with tangentially restrained edges. *Proceedings of the Institution of Mechanical Engineers, Part C: Journal of Mechanical Engineering Science*, 233(9), 3193-3207.

[11] N.V. Tien, V.M. Duc, V.H. Nam, N.T. Phuong, H.S. Lanh, D.T. Dong, L.N. Ly, D. Hung, T.Q. Minh. (2022). Nonlinear Postbuckling of Auxetic-Core Sandwich Toroidal Shell Segments with CNT-Reinforced Face Sheets Under External Pressure. *International Journal of Structural Stability and Dynamics*, 22(1), 2250006.

[12] Y. Wang, R. Zeng, M. Safarpour. (2022). Vibration analysis of FG-GPLRC annular plate in a thermal environment. *Mechanics Based Design of Structures Machines*, 50(1), 352-370.